N. Ohara, Y. Zheng, I. Sato, T. Nakamura and M. Yamaguchi, "Simultaneous linear separation and unmixing of fluorescent and reflective components from a single hyperspectral image," 2016 IEEE International Conference on Image Processing (ICIP), Phoenix, AZ, 2016, pp. 4344-4348, doi: 10.1109/ICIP.2016.7533180

SIMULTANEOUS LINEAR SEPARATION AND UNMIXING OF FLUORESCENT AND REFLECTIVE COMPONENTS FROM A SINGLE HYPERSPECTRAL IMAGE

Naoyuki Ohara, Yinqiang Zheng, Imari Sato, Tomoya Nakamura, Masahiro Yamaguchi

Tokyo Institute of Technology, National Institute of Informatics

ABSTRACT

Recently an algorithm to separate fluorescent and reflective components from a hyperspectral image has been reported, in which the important task of spectral unmixing of multiple fluorescent components was left unresolved. In this paper, we present the algorithm to simultaneously separate those components and unmix fluorophores (SSUF: Simultaneous Separation and Unmixing of Fluorescent components) from a single hyperspectral image. Two variants are introduced for the cases when fluorophore spectra are known and unknown. Experimental results confirm the validity of the proposed method.

Index Terms— fluorescence imaging, hyperspectral imaging, spectral unmixing, reflectrance estimation

1. INTRODUCTION

Fluorescence imaging plays an important role in biomedical field, and recently it is also getting attention in computer vision community. In fluorescence molecular imaging, the use of multiple biomarkers is advantageous for improving accuracy and efficiency. Multispectral fluorescent imaging has been applied to visualize multiple biomarker expressions, and is also needed to adopt spectral unmixing technique for removing the crosstalk [1,2]. For the acquisition of full spectral characteristics of fluorescent objects, the measurement of bispectral matrix, or Donaldson matrix is needed [3], however, it requires large number of observations with changing illuminant spectrum. Recently, algorithms to separate fluorescent and reflective component from small number of hyperspectral images have been reported [4-8]. Especially in [4], only a single hyperspectral image is needed along with the illuminant with peaky spectrum; thus, it will be possible to allow video fluorescence imaging. For the purpose to apply the method to biomedical imaging, which uses multiple biomarkers or autofluorescnece, it is necessary to enable unmixing of fluorescent components or fluorophores. Unmixing of fluorophores will be useful for not only biomedical imaging but also other applications such as pigment mapping of paintings that contain fluorescent components.

Our goal is to separate reflective and fluorescent components and to unmix fluorescent components from a single hyperspectral image. Here, two cases are considered; the cases when spectral characteristics of fluorophores are known and unknown. The proposed method estimates the image of reflective component, the image of the fluorophore amounts (called abundance maps), and the fluorescence emission spectrum of each fluorophore in the case of unknown fluorophore spectra. Although the hyperspectral camera used in this experiment is a pushbroom sensor and captures still-image only, the combination of single-shot hyperspectral camera [7] will enable high-framerate video fluorescence imaging.

Our contribution in this paper is twofold; (1) developed an algorithm to simultaneously separate and unmix fluorescent components (SSUF), (2) as the limitation of linear unmixing, the nonlinear relationship between the abundance and the observed spectra is demonstrated and the results of simple correction method are shown.

In Section 2, we introduce the related work on fluorescence separation, in Section 3, we formulate the problem and the algorithm of the proposed SSUF method, and in Section 4, we show experimental results using synthetic and real data. In Section 5, we summarize this paper.

2. RELATED WORK

Linear unmixing is well-known in fluorescence spectral imaging as a technique to remove cross-talk and auto-fluorescence [1,2]. In conventional spectral imaging of fluorescent objects, multiple images must be acquired with changing illuminant. Recently, some reports deal with the methods to estimate both reflective and fluorescent components with small number of observations [4-8]. Fu et al. succeeded in separating fluorescent and reflective components using programmable light source and two hyperspectral images [5]. Zheng et al. reported a similar method using ordinary illuminants (incandescent, fluorescent, and LED lamps) and 3 hyperspectral images [6]. Later, Zheng et al. showed that the separation is possible by using HID (High Intensity Discharge) lamp and one hyperspectral image [4]. Our proposed SSUF is based on [4].

3. SIMULTANEOUS SEPARATION AND UNMIXING

3.1. Linear mixing model for multiple fluorescence

Consider illuminating an object that has fluorescent and reflective components, and capturing the scene by a hyperspectral camera. The measured radiance spectrum of each pixel can be considered as a linear combination of reflective and fluorescent components. According to [6], the measured spectrum at each pixel can be written as

$$g(\lambda) = l(\lambda)r(\lambda) + se(\lambda) \quad (1)$$

where $g(\lambda)$ is the radiance measured by hyperspectral camera, $l(\lambda)$ is the illuminant spectrum, $r(\lambda)$ is the reflectance, $e(\lambda)$ is the emission spectrum of fluorescence, respectively. $s = \int a(\tilde{\lambda})l(\tilde{\lambda})d\tilde{\lambda}$ is the excitation coefficient where $a(\lambda)$ is the excitation spectrum of fluorescence.

When there are p fluorophores in the scene, Eq. (1) is rewritten as

$$g(\lambda) = l(\lambda)r(\lambda) + \sum_{i=1}^{p} s_i q_i e_i(\lambda) \quad (2)$$

where s_i, q_i and $e_i(\lambda)$ are the excitation coefficient, the fluorescence abundance, and the emission spectrum of i-th fluorophore, respectively.

Equation (2) indicates that if we use different illuminant, the spectral radiance of fluorescent components also changes because s_i depends on the illuminant radiance in the excitation wavelength range of i-th fluorophore. In this work, we consider the use of a single hyperspectral image so as to avoid the change of the fluorescence spectrum.

Let n be the number of bands of a hyperspectral camera. The discrete form of Eq. (2) is given by

$$\mathbf{g} = L\mathbf{r} + ES\mathbf{q} = [L \quad ES]\begin{bmatrix}\mathbf{r}\\ \mathbf{q}\end{bmatrix} \quad (3)$$

where $\mathbf{g} = [g(\lambda_1), \dots, g(\lambda_n)]^T$, $L = diag(l(\lambda_1), \dots, l(\lambda_n))$, $E = [\mathbf{e}_1, \dots, \mathbf{e}_p]$, $\mathbf{e}_i = [e(\lambda_1), \dots, e(\lambda_n)]^T$, $S = diag(s_1, \dots, s_p)$, $\mathbf{r} = [r(\lambda_1), \dots, r(\lambda_n)]^T$, $\mathbf{q} = [\mathrm{q}_1, \dots, \mathrm{q}_p]^T$, respectively.

3.2. Reduction of unknowns

Excitation spectrum $a(\lambda)$ and illuminant spectrum $l(\lambda)$ often have wider bandwidth than that of each band of a hyperspectral camera or a spectrometer. Thus, it is difficult to calculate s accurately even if we have fluorescence spectra data beforehand. Blind estimation of s is also difficult problem because of bilinearity of s and q.

In this paper, we estimate $s_i q_i$ instead of q_i. It corresponds that a_i is assumed to be unity. As a result, eq.(3) can be simplified as follows

$$\mathbf{g} = [L \quad E]\begin{bmatrix}\mathbf{r}\\ \mathbf{q}\end{bmatrix}. \quad (4)$$

Emission spectra $e(\lambda)$ are normalized so that their peaks become 1. Therefore, q_i represents the peak height of the spectral radiance of i-th florescence component.

3.3. Condition number improvement by high-frequency illuminant

The condition number of the matrix $[L \quad E]$ becomes large when illuminant L is ordinary one that has continuous spectral distribution [6]. An illuminant with spiky spectral distribution is used for this purpose so that reflective component has very different shape from emission spectra. As an example of such illuminant is HID, which is used in the experiment below.

3.4. SSUF Algorithm

3.4.1. Case 1: Known fluorescence

First, consider the case that emission spectra E of fluorophores are known. Such condition is not special because spectral data of fluorescent dyes can be easily obtained from a data sheet, or a separate measurement. In this case, $L, E,$ and $\mathbf{g}$ are known, and $\mathbf{r}$ and $\mathbf{q}$ are unknown.

Equation (4) has n equations and $n + p$ variables, thus it is underdetermined.

It is known that spectral reflectance is usually smooth. Incorporating such constraint, a solution can be obtained by solving following quadratic programming problem:

$$\min_{\mathbf{r},\mathbf{q}} \epsilon\|D\mathbf{r}\|_2^2 + \left\|\mathbf{g} - [L \quad E]\begin{bmatrix}\mathbf{r}\\ \mathbf{q}\end{bmatrix}\right\|_2^2 \text{ subject to } \begin{bmatrix}\mathbf{r}\\ \mathbf{q}\end{bmatrix} \geq \mathbf{0}$$

where $\epsilon > 0$ is strength of smoothness, D is second-order differential matrix.

3.4.2. Case 2: Unknown fluorescence

Secondly, consider the case that the scene contains unknown fluorophores. Now, $L, \mathbf{g}$ is known, and $E, \mathbf{r}, \mathbf{q}$ is unknown. The difference from Case 1 is that E is being unknown. In this case, E is estimated by following steps:

(1) Apply the algorithm of [4] to all pixels and obtain mixed fluorescent components $E\mathbf{q}$.
(2) Unmix fluorescence components using a blind spectral unmixing technique such as Vertex Components Analysis (VCA) [10].

Once E is obtained, we can apply the algorithm explained in Sec. 3.4.1.

3.5. Correction of nonlinear effects

Fluorescent emissions are absorbed by other absorbents, and fluorescence abundance is not proportional to the concentration of fluorophore (inner filter effect). There are also non-fluorescent absorbents in the object considered in this work and they affect the excitation light as well. In the following experiment, we applied a simple method for its correction.

When absorption occurs, fluorescent component $E\mathbf{q}$ becomes $RE\mathbf{q}$, where $R = diag(\mathbf{r})$. Thus, fluorescent component cannot express in the form of linear combination of emission spectra. However, emission spectra are usually narrow bandwidth and reflectance has smooth spectra, thus nonlinear effect of R might be considered with a simplified model. We approximate $RE\mathbf{q} \approx EK\mathbf{q}$, where $K = diag(k_1, \dots, k_p)$. k_i represents weakening rate of q_i. k_i is determined by selecting 5 bands around the peak of ith emission spectrum and averaging estimated reflectance. The

corrected fluorescence abundance q_{ci} can be obtained by $q_{ci} = q_i/k_i$.

4. EXPERIMENTS

4.1. Synthetic data

In the first step of the experiments, we applied the proposed SSUF to synthetic data to check its accuracy. As **r**, we used 18 reflectance spectra of Color Checker (Gretag-Macbeth, currently X-Rite). 6 emission spectra were selected from fluorescence database [11].

We designed an optimal illuminant following the method introduced in [4]. As the illuminant spectrum, we used CIE A, D65, and F1 illuminant, and an HID lamp (D2C) used in [4], and optimal illuminant. Each spectrum is normalized such that its maximum becomes 1. Figure 1 shows the spectral distribution of the optimal and D2C HID lamp used in this numerical experiment.

q was randomly selected, in the range from 0 to 0.5. We synthesized **g** 180 times for each illuminant, with the linear model described by Eq. (4). Noise-free and 5% additive noise cases are simulated. Then it was solved according to the method described in Sec. 3.4.1. To evaluate the accuracy, we used relative error of fluorescence abundance and RMSE for reflectance. Figure 2 shows the average estimation error. D2C and optimal illuminants perform well in both fluorescence abundance and reflectance estimations.

In noise-free case, RMSE (root mean square error) of reflectance under D2C is smaller than that of optimal. Most bands of optimal have no energy, thus it is unable to reconstruct reflectance accurately. Through the simulation using the synthetic data, it was confirmed that the reflectance and abundance can be estimated with RMSE < 2~5%.

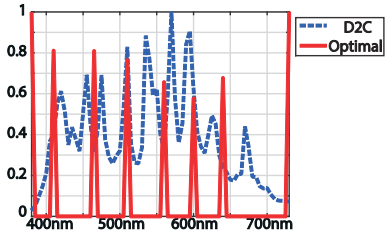

Fig. 1. Spectral distributions of the optimal illuminant and the HID lamp.

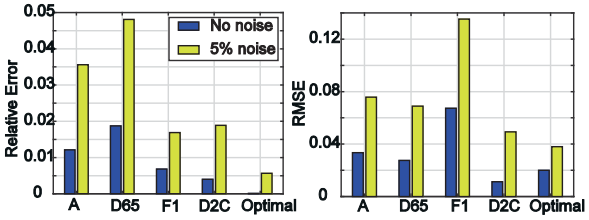

Fig. 2. Estimation accuracy of (left) fluorescence abundance and (right) reflectance.

4.2. Real data

The experimental setup is shown in Fig. 3. Two flat samples were prepared; color patches painted by 2 fluorescence pens (Mitsubishi Pencil PUS-102T and PILOT SGR-8SL-P) and 1 non-fluorescence pen (ZEBRA WYT5-LB). Shorten notations of these pens are FL1, FL2, and NF, respectively. These samples are shown in the first row of Fig. 5. D2C lamp used in [4] was used as illuminant. The sample was illuminated from the front side. The images were captured by using EBA Japan NH-7 Hyperspectral Camera. We used 57 bands from 420nm to 700nm in the hyperspectral images.

Fig. 3. (left) Experimental setup and (right) fluorescent and non-fluorescent pens

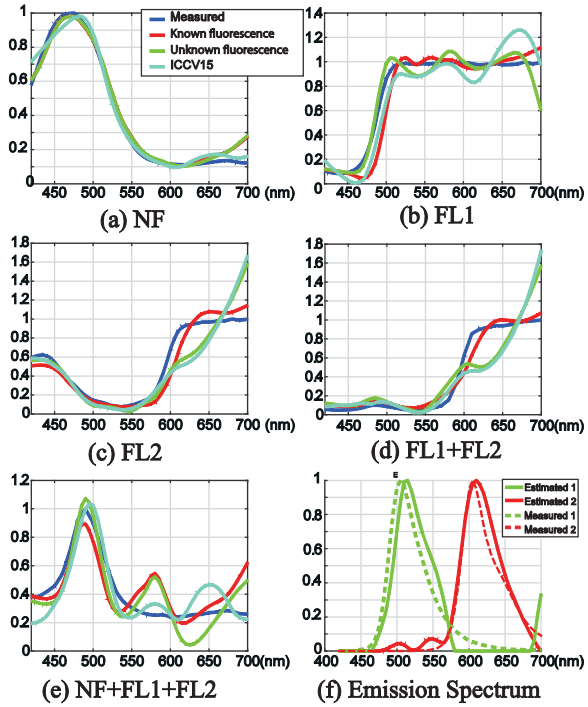

Fig. 4. Estimated reflectance. (a) – (e) indicate the results of the regions of corresponding symbols. (f) Emission spectra of two fluorophores; estimated and measured results.

	(a)	(b)	(c)	(d)	(e)
Known	0.043	0.11	0.10	0.070	0.14
Unknown	0.043	0.086	0.18	0.20	0.13
ICCV15	0.038	0.13	0.21	0.22	0.11

Table 1. RMSE between measured reflectances and estimated ones of three algorithms in (a)-(e) in Fig. 4.

4.2.1 Evaluation of reflectance

We measured the reflectances of 5 regions of the sample shown in Fig. 5 by monochrometer and spectrometer as the reference. In this experiment, the reflectance was estimated under the conditions of known fluorescence and unknown fluorescence. For comparison, the method of [4] (labelled "ICCV15") was applied as well.

The measured and estimated reflectances are also shown in Fig. 4. In NF region, all methods yielded the reflectance spectra with good accuracy. The proposed SSUF worked well even though the pixel did not contain fluorescence.

In FL1 region, all algorithms gave mostly good results, though unknown case and ICCV15 looks slightly unstable. In FL2 and FL1+FL2 regions, the known fluorescence case achieves good accuracy, but in the unknown case and ICCV15, the error became large in the wavelength range longer than 600nm. The estimation of reflectance was sensitive to the estimation of emission spectra. In NF+FL1+FL2 region, all algorithms yielded similar accuracy, but oscillation was observed in the reconstructed spectrum. It was probably because this region had low reflectance and the SNR was poor.

RMSE between measured reflectances and estimated ones of are shown in Table 1. In (c) and (d), known case is evidently better than others. RMSE of unknown case is about as small as ICCV15.

4.2.2 Evaluation of estimated images

Estimation results of reflectance and abundance are shown in Figs. 5. Under both known and unknown fluorescence condition, resultant images looks similar.

The estimated fluorescence abundance of FL1 in the regions overlapping with NF and/or FL2 is smaller than the other regions with FL1 only. As for the FL2 abundance, the estimation in regions overlapping with FL1 is larger, and the estimation in the regions overlapping with NF is smaller than the FL1 only regions. It is known as "inner filter effect," and 3 factors are considered as the causes of these phenomena:

1. Fluorescent component is absorbed by other materials.
2. Illuminant is absorbed by other materials, resulting in weaker excitation.
3. Fluorophore is excited by the emitted light by another fluorophore.

The results of correction algorithm explained in Section 3.5 are also shown in Fig. 5. It can be reduced by the correction, which is not sufficient though, because the correction method can deal with the effect of only the first phenomenon.

5. CONCLUSION

This paper presented a method for simultaneously separating reflective and fluorescence components and unmixing the multiple fluorophore components, from a single hyperspectral image captured under a special illuminant. The proposed method successfully separated and unmixed the fluorescence and reflective components. We observed nonlinearity due to the interaction of fluorescence and absorption, and a simple algorithm was applied to correct the nonlinear effect. The correction is still not sufficient.

As the future work, more detailed quantitative evaluation is needed. Moreover, the proposed SSUF will be implemented with a single-shot hyperspectral camera as well as the hyperspectral video system.

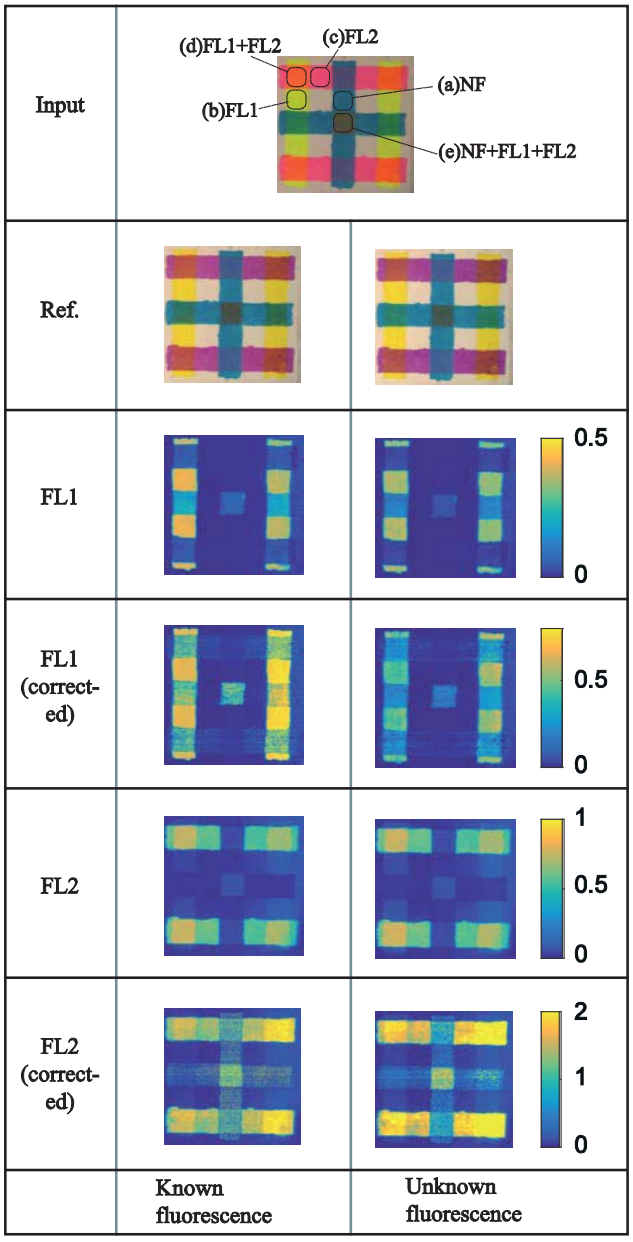

Fig. 5. The estimation results. "Input" row shows the captured image with the explanation of the paintings. "Ref." row is showing the estimated reflectance maps by color images. FL1 and FL2 rows correspond to the estimated abundance maps of FL1 and FL2, respectively, and those with "(corrected)" are the results corrected by the method explained in Section 3.5.

REFERENCES

[1] R. M. Levenson, and J. R. Mansfield, "Multispectral imaging in biology and medicine: Slices of life," *Cytometry, 69A*: 748–758, 2006.

[2] B. Kraus, M. Ziegler, H. Wolff, "Linear fluorescence unmixing in cell biological research," in *Modern Research and Educational Topics in Microscopy*, FORMATEX, 863-872, 2007.

[3] R Donaldson, "Spectrophotometry of fluorescent pigments," *British Journal of Applied Physics*, Vol. 5, 6, 210-214, 1954.

[4] Y. Zheng, Y. Fu, I. Sato, and Y. Sato, "Separating Fluorescent and Reflective Components by Using a Single Hyperspectral Image," in *Proc. IEEE International Conference on Computer Vision (ICCV)*, pp. 3523-3531, 2015.

[5] Y. Fu, A. Lam, I. Sato, T. Okabe, and Y. Sato, "Separating Reflective and Fluorescent Components Using High Frequency Illumination in the Spectral Domain," in *Proc. IEEE International Conference on Computer Vision (ICCV)*, pp. 457-464, 2013.

[6] Y. Zheng, I. Sato, and Y. Sato, "Spectra estimation of fluorescent and reflective scenes by using ordinary illuminants," in *European Conference on Computer Vision (ECCV)*, pp. 188-202, 2014.

[7] J. Mutanen, J. Kinnunen, M. Yamaguchi, and N. Ohyama, "New Method for Reproducing Fluorescent Colors," *CGIV/MCS 2008*: 564-569, 2008.

[8] S. Tominaga, K. Hirai, and T. Horiuchi, "Estimation of bispectral Donaldson matrices of fluorescent objects by using two illuminant projections," *J. Opt. Soc. Am. A 32*, 1068-1078, 2015.

[9] Y. Murakami, K. Nakazaki, and M. Yamaguchi, "Hybrid-resolution spectral video system using low-resolution spectral sensor," *Opt. Express 22*, 20311-20325, 2014.

[10] J.M.P. Nascimento, and J.M.B Dias, "Vertex Component Analysis: A Fast Algorithm to Unmix Hyperspectral Data," *IEEE Transactions on Geoscience and Remote Sensing*, pp. 898-910, 2005.

[11] "Spectra Database hosted at the University of Arizona," http://www.spectra.arizona.edu/